HAL
open science

Non-intersection exponents of fully packed trails on the square lattice

Yacine Ikhlef, Jesper Lykke Jacobsen, Hubert Saleur

To cite this version:

Yacine Ikhlef, Jesper Lykke Jacobsen, Hubert Saleur. Non-intersection exponents of fully packed trails on the square lattice. Journal of Statistical Mechanics: Theory and Experiment, 2007, pp.P05005. hal-00119655v2

HAL Id: hal-00119655

https://hal.science/hal-00119655v2

Submitted on 9 May 2007

HAL is a multi-disciplinary open access archive for the deposit and dissemination of scientific research documents, whether they are published or not. The documents may come from teaching and research institutions in France or abroad, or from public or private research centers.

L'archive ouverte pluridisciplinaire **HAL**, est destinée au dépôt et à la diffusion de documents scientifiques de niveau recherche, publiés ou non, émanant des établissements d'enseignement et de recherche français ou étrangers, des laboratoires publics ou privés.

Non-intersection exponents of fully packed trails on the square lattice.

Yacine Ikhlef[1,2], Jesper Jacobsen[1,2] and Hubert Saleur[2,3]

[1] LPTMS, Université Paris-Sud, Bâtiment 100,
Orsay, 91405, France
[2] Service de Physique Théorique, CEA Saclay,
Gif Sur Yvette, 91191, France
[3] Department of Physics and Astronomy, University of Southern California,
Los Angeles, CA 90089, USA

May 9, 2007

hal-00119655, version 2 - 9 May 2007

Abstract

Fully packed trails on the square lattice are known to be described, in the long distance limit, by a collection of free non compact bosons and symplectic fermions, and thus exhibit some properties reminiscent of Brownian motion, like vanishing fuseau exponents. We investigate in this paper the situation for their non-intersection exponents. Our approach is purely numerical, and based both on transfer matrix and Monte Carlo calculations. We find some evidence for non-intersection exponents given by CFT formulas similar to the Brownian case, albeit slightly different in their details.

1 Introduction

The study of conformally invariant random curves embedded in two-dimensional space has a long history in theoretical physics and probability theory. Recently the subject has gained new momentum due to the advent of a set of rigorous methods known under the name of Stochastic Loewner Evolution (SLE).

Two classes of random curves have been especially well studied. In the first class one finds self-avoiding and mutually avoiding curves, which come in several variants depending on their precise microscopic definition, and in particular whether they occupy a finite fraction of space in the continuum limit. These curves admit a height representation (roughly speaking, using the curves as level lines of the height) and as such are amenable to the use of Coulomb Gas (CG) techniques. Also, the corresponding (twisted) vertex models can be studied as quantum spin chains, *i.e.*, using Bethe Ansatz (BA). As a result, the bulk critical behaviour of self-avoiding curves is very well understood, whereas important questions regarding their surface behaviour still remain open [1]. Many of the exact results obtained by the CG route have recently been confirmed, or extended, by the SLE approach.

The second example of random curves is that of Brownian motion, which is best studied directly in the continuum limit. Profound links exist between this and the foregoing case, *via* the use of SLE [2] or quantum gravity [3] methods. To give but one example, the external hull of the Brownian curve turns out to be in the universality class of the (standard, dilute) self-avoiding walk [3]. On a microscopic level, however, there are two crucial differences. First, a Brownian motion can intersect itself, making the application of height mappings and CG techniques break down.

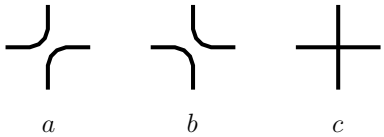

Figure 1: The three allowed vertices in the Brauer loop model, with weights $1, 1, x$.

Second, it can pass through the same site an infinite number of times, making it more difficult to use the BA approach [1].

As a result, up to this day, the non-intersection exponents for Brownian motion, which were identified by Duplantier and Kwon [5, 3] twenty years ago, and whose values were rigorously established recently [2], cannot be derived using the BA or variants of the CG method applied directly to a suitable discrete lattice model in flat space.

The present work started with the recent discovery of lattice models that bear a close resemblance to Brownian motion, yet are tractable by the usual techniques. These models are what is sometimes called *dense trails*, and can be obtained by allowing self-intersections as well as mutual intersections in a dense loop gas, while still requiring that the curves pass through each lattice link (resp. site) once (resp. twice) at the most. The introduction of such intersections is well known not to change the universality class in the dilute case, but—surprisingly maybe—does affect it profoundly in the dense case (for an early discussion see [6]). It was in particular argued in [7] that for such a model with a loop fugacity $n < 2$, all the fuseau exponents vanish exactly, and the corresponding correlation functions are described by non compact bosonic fields, exactly like in the pure Brownian case. This was checked analytically and numerically in the case of fully packed trails (also called *Brauer loop model*) [8, 7].

It is of course tempting to ask how close fully packed trails and Brownian motion actually are, and a natural route to investigate this question is to study the non-intersection exponents.

Fully packed trails, or Brauer loop models, depend among other things on the fugacity n of loops. We will concentrate here on the case $n = 0$ (hence, of a single trail), but notice that the case $n = 1$ has recently been studied numerically by Kager and Nienhuis [9]. These authors found that the hull distribution was compatible with that of a reflected Brownian motion. In our work, we define a scale-invariant "escape path" Γ within a Brauer loop model with fugacity $n = 0$. Our main findings are that while the fractal dimension of Γ agrees (marginally) with that of the self-avoiding walk, the non-intersection exponents are definitely different from those of [5, 2], though might well be given exactly by a related formula.

The paper is organized as follows. In section 2 we define precisely the model of fully packed trails to be studied, and in section 3 we introduce the escape path Γ and discuss how it can be made scale invariant. A qualitative phase diagram is established in section 4. Finally, the non-intersection exponents and the scaling properties of Γ are measured using transfer matrix (section 5) and Monte-Carlo (section 6) techniques. We give our conclusions in section 7.

2 Brauer loop model on the square lattice

We consider, on the square lattice, the *Brauer loop model* defined by the three vertices a, b and c, shown in figure 1. The local Boltzmann weights are given by :

$$\omega_a, \omega_b, \omega_c = 1, 1, x \tag{1}$$

We give an additional weight n for each closed loop.

[1] We note that there has been some important progress recently [4] in the study of Bethe Ansatz for statistical mechanics systems with an infinite number of degrees of freedom per site in relation with quantum spin chains on non compact groups.

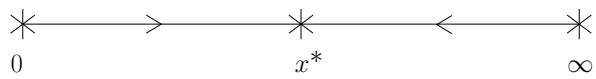

Figure 2: Renormalization flow of the loop model, for the parameter x.

The renormalization flow for the parameter x is shown in figure 2. The fixed point $x = 0$ corresponds, for $-2 \leq n \leq 2$, to the low-temperature phase of the $O(n)$ model [10]. The fixed point x^* attracts, for integer [7] and presumably also real values of n, all the points in the phase $x > 0$. This phase contains an integrable point $x_{\text{int}} = (1 - n/2)/2$ [8]. At this particular value of x, the R-matrix (expressed in the connectivity basis) satisfies the Yang-Baxter equations for any real value of n.

The goal of this paper is to study the non-intersection properties of the Brauer loop model. Recall that in the Brownian case, the simplest such property is the disconnection exponent, which governs the probability that the origin of a single Brownian path remains accessible from infinity without the path being crossed. Let us recall some of the well established results in this case. If one considers a random walk of length S, the origin stays connected to infinity with probability $P(S) \sim S^{-\zeta_1}$, with $\zeta_1 = 1/8$. One can also imagine growing the walk until it reaches the circle of radius R, and ask the probability with which it has left the origin connected to infinity, in which case $P(R) \sim R^{-2\zeta_1}$. Finally, one can consider a two-point correlation function defined as the weighted sum [5] over all walks going from the origin to a point $\mathbf{r}$ for which either extremity remains connected to infinity. When the monomer fugacity equals the critical value, $G(\mathbf{r}) \sim |\mathbf{r}|^{-2x_1}$ with $x_1 = 2\zeta_1 = 1/4$.

By analogy, we define an *interface* as a line (of arbitrary length) that the Brauer loops are not allowed to cross. In particular, we adress the following problems :

1. Define the above loop model on a finite lattice of N sites. Let the origin 0 be a point inside the lattice, and $\mathbf{r}$ a point on the boundary of the lattice. Let $P(\mathbf{r})$ be the probability that there exists an interface going from the origin to the point $\mathbf{r}$. How does $P(\mathbf{r})$ decay when $r = |\mathbf{r}|$ goes to infinity ?

2. When this interface exists, it is, by definition, a self-avoiding walk—for easy reference we henceforth refer to it as Γ. The original loop system around Γ acts like an environment, affecting its geometrical properties. What is the universality class of Γ ?

3 Definition of a fluctuating interface

It turns out that in the Brauer loop model with a single loop, for any $x > 0$, the probability $P(\mathbf{r})$ behaves as :

$$P(\mathbf{r}) \sim \exp(-r/\xi) \tag{2}$$

where ξ is a length-scale depending on x. This behaviour is profundly different from the one of Brownian motion, where the probability $P(\mathbf{r})$ for a long Brownian trajectory decays algebraically (a consequence of subadditivity arguments [11]). This indicates that, without modification, the interfaces in the Brauer model at $n = 0$ do not have interesting scaling properties.

Let us see more explicitely why such behaviour arises. Define three partition functions $Z_0(N)$, $Z'(N|0, \mathbf{r})$ and $Z_0(N|\Gamma)$ as follows.

- Let $Z_0(N)$ be the partition sum of the loop model for N sites.

- Let $Z'(N|0,\mathbf{r})$ be the partition sum of the loop model with the constraint that there exists an interface not crossed by the loop, going from 0 to $\mathbf{r}$. When a loop configuration admits an interface Γ, then this interface is unique (or else there would be several loops). Thus, one can rewrite the sum $Z'(N|0,\mathbf{r})$ by grouping the terms corresponding to the same interface Γ :

$$Z'(N|0,\mathbf{r}) = \sum_{\Gamma \in \mathrm{SAW}(0,\mathbf{r})} Z_0(N|\Gamma) \tag{3}$$

  where $\mathrm{SAW}(0,\mathbf{r})$ is the set of all self-avoiding walks with ends fixed to 0 and $\mathbf{r}$, and $Z_0(N|\Gamma)$ is the partition sum of the loop model with the interface defined by the self-avoiding walk configuration Γ.

Consider the presence of an effective interface energy in $Z_0(N|\Gamma)$:

$$Z_0(N|\Gamma) \sim Z_0(N)\ \exp[-l \times F_s(x)] \tag{4}$$

where l is the length of Γ, and F_s is a free energy per unit of length of Γ. The number of self-avoiding walk configurations of length l is approximately $(\mu_{\mathrm{SAW}})^l$, where $\mu_{\mathrm{SAW}} = 2.6381(5)$ [12] is the connectivity constant of self-avoiding walks on the square lattice. If the quantity $(F_s - \log \mu_{\mathrm{SAW}})$ is positive, then the behaviour of $Z'(N|0,\mathbf{r})$ is governed by configurations where the interface has minimal length :

$$l \simeq r \tag{5}$$

$$Z'(N|0,\mathbf{r}) \sim Z_0(N)\ \exp[-(F_s - \log \mu_{\mathrm{SAW}})r] \tag{6}$$

This accounts for the exponential behaviour of $P(\mathbf{r}) = Z'(N|0,\mathbf{r})/Z_0(N)$.

In order to define a scale-invariant interface, we need to allow its length l to develop big fluctuations. A simple way to do this is to introduce an additional Boltzmann weight w^l, where l is the length of Γ. Thus, we are interested in the study of the partition function :

$$Z(N|0,\mathbf{r}) \equiv \sum_{\Gamma \in \mathrm{SAW}(0,\mathbf{r})} w^l Z_0(N|\Gamma) \tag{7}$$

This function contains two external parameters : x, the fugacity of a crossing in the loop model defined by $Z_0(N|\Gamma)$; and w, that controls the length l of the interface Γ. A typical configuration contributing to the partition sum (7) is shown in figure 3.

4 Phase diagram

Using renormalization group arguments and anticipating on our numerical and analytical results, we try to give a consistent picture of the phase diagram of the model defined by equation (7).

Let us fix the value of $x \geq 0$, and observe the system as we vary w. In this picture, the interface Γ is a self-avoiding walk, with its self-interactions induced by the surrounding loop model. According to equation (4), we expect a phase transition at $w^*(x) = \exp[F_s(x)]/\mu_{\mathrm{SAW}}$.

Note that it may be possible to check the previous relation. We can compute numerically the value of w^*. If we could also compute independently the value of F_s, then we would be able to compare these values with the connectivity constant μ_{SAW}, which is a well-known constant [12].

Given w^*, the qualitative behaviour of the system as a function of w is expected to be as follows :

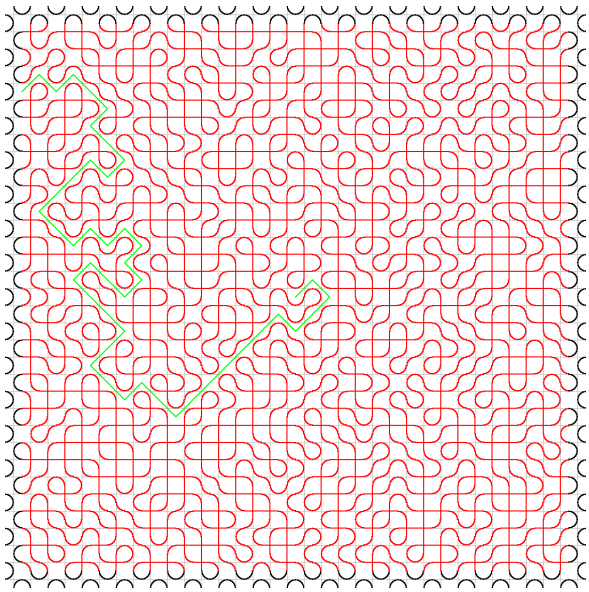

Figure 3: A typical configuration contributing to the partition sum $Z(N|0,\mathbf{r})$.

- If $w < w^*$, the behaviour of $Z(N|0,\mathbf{r})$ is governed by configurations where the interface has minimal length : this phase is "non-critical" from the point of view of the interface. The statement (2) amounts to the inequality : $w^* > 1$, for every $x > 0$. In the phase $w < w^*$, the interface acts as a non-fluctuating boundary for the loop model. So we expect the points of this phase to flow towards one of the fixed points described in section 2.

- If $w = w^*$, the interface length l fluctuates above its minimal value r, with fluctuations of the order of the system size. It is a fractal object, with Hausdorff dimension $1 < d_f \leq 2$. We call this point the "Γ-dilute" critical point.

- If $w > w^*$, two scenarii, illustrated in figure 4, are possible *a priori*. In scenario 1, there exists a fixed point w_D such that $w^* < w_D < \infty$, and the whole phase flows towards it. In scenario 2, no such fixed point exists, and the whole phase flows towards the point $w = \infty$. Numerical studies suggest that scenario 1 is correct.

This behaviour with respect to w is very similar to the one of ordinary self-avoiding walks when driven into the dense phase by a large monomer fugacity [13]. The interface Γ plays the role of the single chain, and the parameter w is the monomer fugacity for the chain Γ.

To summarize, the phase diagram is given in figure 5. The points (1) and (2) are the critical points of the intersecting loop model with a fixed boundary. The point (3) (*resp.* (4)) is the "Γ-dilute" point for $x > 0$ (*resp.* $x = 0$). The point (5) (*resp.* (6)) is the "Γ-dense" point for $x > 0$ (*resp.* $x = 0$). The line passing through (3) and (4) has equation : $w = w^*(x)$.

Let us focus on the critical point (4). Since $x = 0$, only vertices of type a and b are allowed, and the point (4) is equivalent to the Q-state Potts model on the square lattice, in a particular limit : in the Fortuin-Kasteleyn formulation, a cluster has fugacity $Q \to 0$ and a bond has fugacity $v = \sqrt{Q}$. The leading term of the partition sum describes equiprobable spanning trees. In this context, the interface Γ is exactly the set of *red bonds* of the spanning

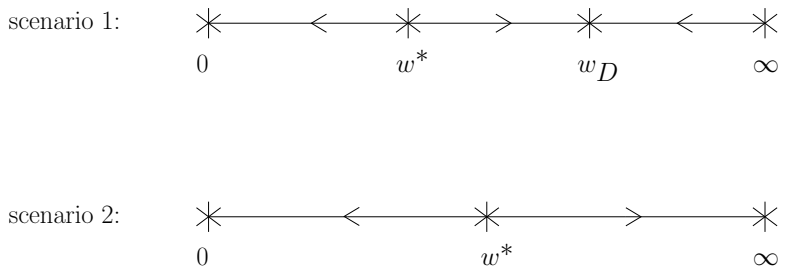

Figure 4: Two scenarii for the flow diagram of the parameter w. Numerical studies suggest that scenario 1 is correct.

tree (the red bonds are the bonds of the spanning tree which disconnect 0 from $\mathbf{r}$ if removed). The fractal dimension of this object is 5/4 [14, 15].

The point (2) is just equivalent to the Q-state Potts model in the limit described above, with a fixed cut line uncrossed by the loop.

5 Transfer matrix formulation

5.1 Mapping from the plane onto the cylinder

In order to estimate partition sums such as $Z_0(N)$, $Z(N|0,\mathbf{r})$ on a cylinder of fixed width L and length $M \to \infty$, we compute the leading eigenvalues of the transfer matrix. Denote them $\Lambda_L^{(0)}, \Lambda_L^{(1)}, \Lambda_L^{(2)}, \ldots$ in decreasing order of modulus. Then the eigenvalue $\Lambda_L^{(i)}$ defines the free energy density by surface unit $f_L^{(i)}$ in the following way :

$$Z_{\rm cyl}^{(i)}(M,L) \sim \left(\Lambda_L^{(i)}\right)^M \tag{8}$$

$$f_L^{(i)} = \frac{1}{ML}\log Z_{\rm cyl}^{(i)}(M,L) \sim \frac{1}{L}\log \Lambda_L^{(i)} \tag{9}$$

For conformally invariant models, finite-size corrections to $f_L^{(i)}$ give access to the central charge c and to the operator dimensions $X^{(i)}$ [16, 17] :

$$f_L^{(0)} = f_\infty + \frac{\pi c}{6L^2} + o(L^{-2}) \tag{10}$$

$$f_L^{(0)} - f_L^{(i)} = \frac{2\pi X^{(i)}}{L^2} + o(L^{-2}) \tag{11}$$

where the dimensions are defined in plane geometry by :

$$Z_{\rm pl}^{(i)}(0,\mathbf{r})/Z_{\rm pl}^{(0)} \sim 1/r^{2X^{(i)}} \tag{12}$$

5.2 Transfer matrix for the loop model

Our convention is a transfer matrix T_L acting in the vertical direction, from bottom to top. Let the width L of the cylinder be an even integer. Consider the strands living on the vertical edges of the lattice. A *row configuration* is a

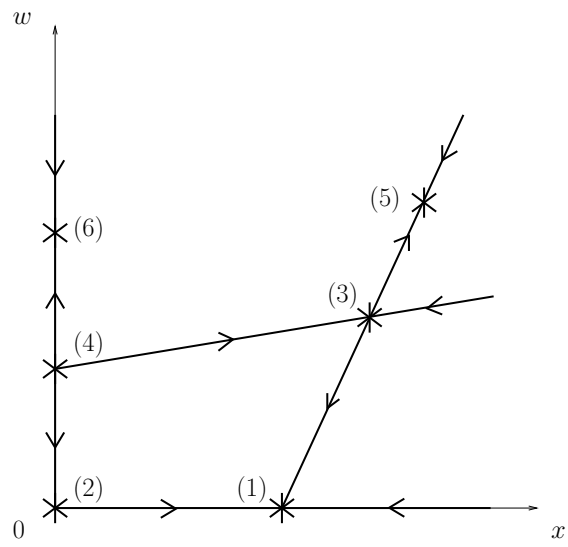

Figure 5: Phase diagram of the model with $n = 0$, in the $x - w$ plane.

pairing of these strands. There are $(L-1)!! = 1 \times 3 \times 5 \times \ldots (L-1)$ pairings of L objects. If α and β are two row configurations, then the matrix element $(T_L)_{\beta\alpha}$ is the total Boltzmann weight of L-vertex configurations that map α to β (see figure 6). This Boltzmann weight includes a factor n each time a loop is closed.

On a cylinder of length M, the partition sum is given by :

$$Z_{0,\mathrm{cyl}}(M, L) = \langle \alpha_{\mathrm{out}} | \, (T_L)^M \, | \alpha_{\mathrm{in}} \rangle \sim \left(\Lambda_L^{(0)} \right)^M \tag{13}$$

where $|\alpha_{\mathrm{in}}\rangle$ and $|\alpha_{\mathrm{out}}\rangle$ are two particular vectors coding the closing of the loop at each extremity of the cylinder. For example, one may choose to close the loop as illustrated in figure 7.

5.3 Definition of an interface on the cylinder

Let Γ be an interface connecting a point A on the bottom circle of the cylinder to a point B on the top circle of the cylinder (see figure 8). Let $Z_{0,\mathrm{cyl}}(M, L|\Gamma)$ be the partition sum of the loop model constrained by the interface Γ.

Define, as in equation (7), the partition sum $Z_{\mathrm{cyl}}(M, L)$:

$$Z_{\mathrm{cyl}}(M, L) \equiv \sum_{\Gamma} w^l \, Z_{0,\mathrm{cyl}}(M, L|\Gamma) \tag{14}$$

Note that the vector $(T_L)^M \, |\alpha_{\mathrm{in}}\rangle$ may contain components on configurations which admit several interfaces. This is because connectivity states are defined by unclosed loop segments. In contrast, the final scalar product (13) contains only contributions from single closed loop configurations admitting exactly one interface.

An analog observation can be done in the plane geometry. Suppose the system is defined on a finite square of $N = L^2$ sites. A given loop configuration contributing to the partition sum $Z(N|0, \mathbf{r})$ admits one and only one interface

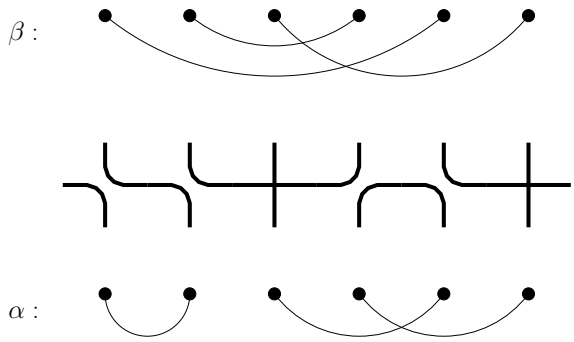

Figure 6: An example term in the matrix element $T_{\beta\alpha}$ of the transfer matrix.

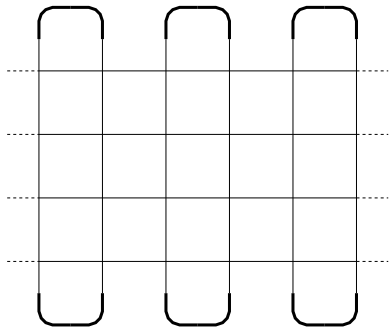

Figure 7: Closing of the loop at the two boundaries of the strip. Dashed lines indicate periodic boundary conditions.

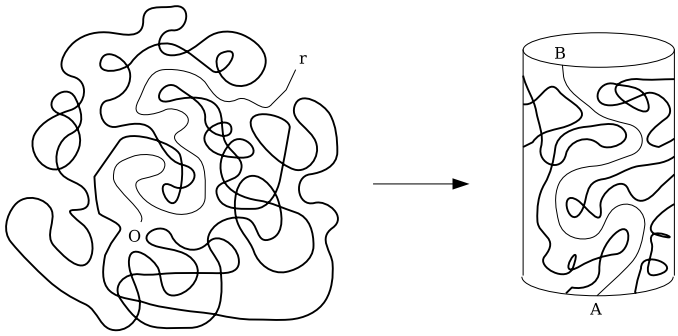

Figure 8: Mapping of the interface problem from the plane to the cylinder.

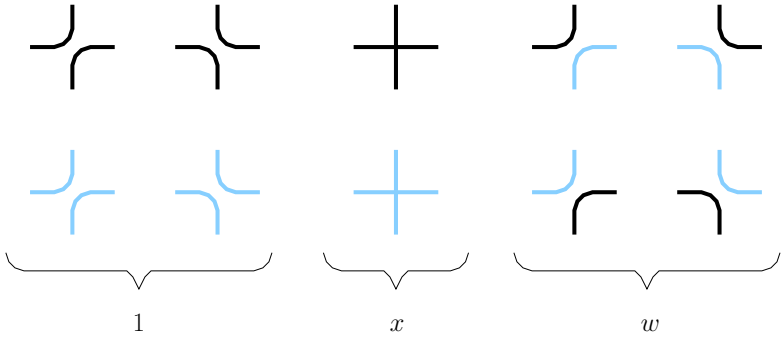

Figure 9: Vertex weights in the colored loop model.

Γ going from 0 to a point of the boundary. But if one considers the subsystem contained in a smaller square centered on 0 and of side $L' < L$, one may find several interfaces going from the origin to a point of the smaller square.

5.4 A local model for the interface weight

The existence of the interface Γ and its weight w^l are non-local features, which can fortunately be expressed by local constraints on a colored loop model with loop fugacity $n = 0$. The loops may take two colors, according to the rules :

- vertices of type (a) and (b) involve two strands of any colors, but vertices of type (c) must involve two strands of the same color.
- the vertex weights are those given in figure 9.
- a strand must change its color when it crosses a seam going along the cylinder.

The loop model defined by these rules satisfies the following properties :

- Every colored loop configuration on the cylinder admits exactly one interface.
- If a loop configuration admits a unique interface, then it can be colored in exactly two ways.
- The interface length l is equal to the number of vertices which involve two different colors.

Thus the partition function of the colored loop model is equal (up to a constant factor) to the partition function $Z_{\text{cyl}}(M, L)$.

5.5 Other partition sums

In the previous discussion we described the partition sum of one loop with one interface. However, the colored loop model allows us to compute partition sums with up to two interfaces, and/or containing open trails.

The trick used to impose the presence of two interfaces is simply to eliminate the color change across the infinite seam.

Open trails are introduced in a standard way into the connectivity basis, by adding states where one or more points are connected to a “virtual” partner. The additional rule is that these points cannot be connected with each other.

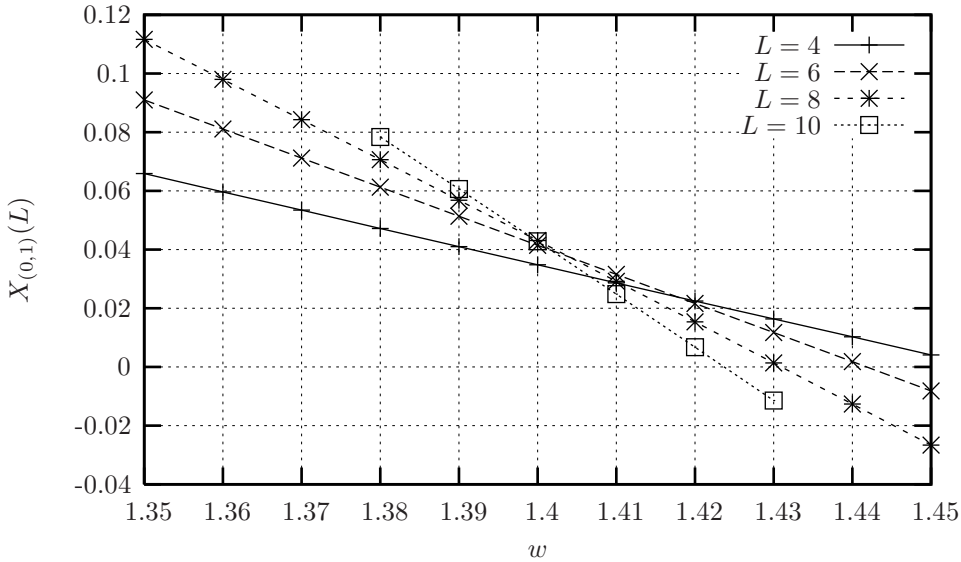

Figure 10: Estimates of the exponent $X_{(0,1)}$ for $x = 1$.

Denote n_1 the number of open trails and n_2 the number of closed loops. The cylinder circumference L must have the same parity as n_1. The partition sums which we are able to reach with the colored loop model have $n_1 + n_2 \leq 2$ interfaces. The corresponding physical exponent is denoted $X_{(n_1,n_2)}$.

5.6 Numerical results

Our numerical procedure is to diagonalize the transfer matrix of the colored loop model, using the power method. Define the exponent $X_{(0,1)}$ by :

$$\frac{Z_{\mathrm{pl}}(N|0,\mathbf{r})}{Z_{0,\mathrm{pl}}(N)} \sim \frac{1}{r^{2X_{(0,1)}}} \tag{15}$$

Using equation (11), we define the finite-size estimates $X_{(0,1)}(L)$ by :

$$X_{(0,1)}(L) \equiv \frac{L^2}{2\pi}\left(f_L^{(0)} - f_{L,(0,1)}\right) \tag{16}$$

These estimates are also useful to determine the position of the critical point w^*. Indeed, consecutive estimates $X_{(0,1)}(L)$ and $X_{(0,1)}(L+2)$ coincide at $w = w^*(L, L+2)$, and—by analogy with standard phenomenological renormalisation group methods—we expect this value to converge to w^* when L is large. This method is illustrated in figure 10. The resulting critical line is plotted in figure 11.

Following a similar method, we define the general exponent $X_{(n_1,n_2)}$ by comparing the free energy $f_{L,(n_1,n_2)}$ with the free energy associated with the greatest eigenvalue for the same system width :

$$X_{(n_1,n_2)}(L) \equiv \frac{L^2}{2\pi}\left(f_L^{(0)} - f_{L,(n_1,n_2)}\right) \tag{17}$$

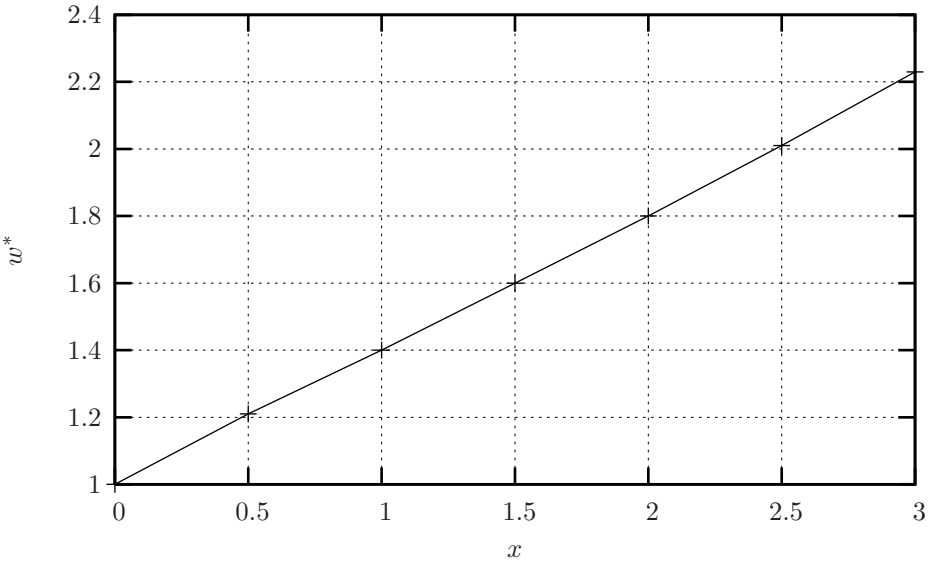

Figure 11: Position of the critical point w^* as a function of x. The values were obtained for width $L = 8, 10$. The curve is very well approximated by the formula : $w^* = 1 + 0.4\ x$.

Note that $f_L^{(0)}$ is the free energy of one unconstrained loop (*resp.* trail) when L is even (*resp.* odd).

The errorbars are given by the spacing of the consecutive intersections of the finite-size estimates. The results are compared with the empirical formula :

$$X_{(n_1,n_2)} = \frac{m^2-1}{12}, \qquad m = \frac{3}{2}n_1 + 2n_2 - 1 \tag{18}$$

to be discussed in the last section.

One must consider these results cautiously, because in the loop model, logarithmic corrections appear in quantities such as $f_L^{(0)}$.

Name	Description	Numerical	Formula (18)
$X_{(0,1)}$	1 loop, 1 interface	0.04 ± 0.005	0
$X_{(1,0)}$	1 trail, 1 interface	0.00 ± 0.005	-0.06
$X_{(0,2)}$	2 loops, 2 interfaces	0.80 ± 0.02	0.67
$X_{(1,1)}$	1 loop, 1 trail, 2 interfaces	0.50 ± 0.008	0.44
$X_{(2,0)}$	2 trails, 2 interfaces	0.21 ± 0.02	0.25

Table 1: Estimates of the exponents $X_{(n_1,n_2)}$ by transfer-matrix diagonalisation.

6 Monte-Carlo simulation on a square

In order to access directly some geometrical features of the model, we simulate it by a Monte-Carlo procedure [18] on an $L \times L$ square lattice. First, we describe a Metropolis procedure used for the loop model defined by the partition sum $Z_0(N)$. Then, we modify slightly this procedure to simulate the ensemble defined by $Z(N|0, \mathbf{r})$. We discuss the main aspects of the algorithm : detailed balance, ergodicity and autocorrelation times. At the end, we give some numerical results obtained by this method.

6.1 Metropolis procedure for the loop model

The statistical ensemble of interest is the set of loop configurations consisting of *exactly one loop* on an $L \times L$ square lattice. Each loop configuration $\mathcal{L}$ is given the Boltzmann weight $\Pi(\mathcal{L}) = x^{N_c}$, where N_c is the number of crossings of the loop with itself. The boundary of the square consists of "frozen" vertices, as shown in figure 3.

The idea of the algorithm is to modify locally the system without violating the one-loop constraint. Let us denote P_{ij} the 2×2 "plaquette" consisting of the vertices $\{(i,j),(i+1,j),(i,j+1),(i+1,j+1)\}$, and β_{ij} the state of these four vertices. Every plaquette has eight "external legs". Outside P_{ij}, the loop connects these legs with each other. Fixing this external connectivity—call it α—defines the set B_α of plaquette configurations β respecting the one-loop constraint when adjoined with α.

An elementary iteration consists of four steps :

1. Pick uniformly a plaquette P among $(L-1) \times (L-1)$ possibilities. The state of the plaquette is denoted β.
2. Visit the loop to determine the external connectivity α of the legs of P.
3. Pick uniformly a configuration β' from B_α.
4. Perform the local change $\beta \to \beta'$ on P with probability :

$$W(\beta \to \beta') = \begin{cases} \frac{\Pi(\beta')}{\Pi(\beta)} & \text{if } \Pi(\beta') < \Pi(\beta) \\ 1 & \text{otherwise} \end{cases} \tag{19}$$

This algorithm satisfies the detailed balance condition for the probability distribution $\Pi(\mathcal{L})$ on the set of one-loop configurations :

$$\forall \mathcal{L}, \mathcal{L}' \quad \Pi(\mathcal{L}) W(\mathcal{L} \to \mathcal{L}') = \Pi(\mathcal{L}') W(\mathcal{L}' \to \mathcal{L}) \tag{20}$$

6.2 Metropolis procedure for the loop model with an interface

Consider next the statistical ensemble of one-loop configurations admitting an interface Γ that connects the center O of the square to a point $\mathbf{r}$ on the boundary of the square (see figure 3). Each loop configuration is given the weight $\Pi(\mathcal{L}) = x^{N_c} w^l$, where N_c is the number of crossings of the loop with itself, and l is the length of the interface Γ. The above Metropolis procedure can be adapted to simulate this ensemble, and is defined by the elementary iteration :

1. Pick uniformly a plaquette P among $(L-1) \times (L-1)$ possibilities. The state of the plaquette is denoted β.
2. Visit the loop to determine the external connectivity α of the legs of P.
3. Pick uniformly a configuration β' from B_α. This defines a new loop configuration.

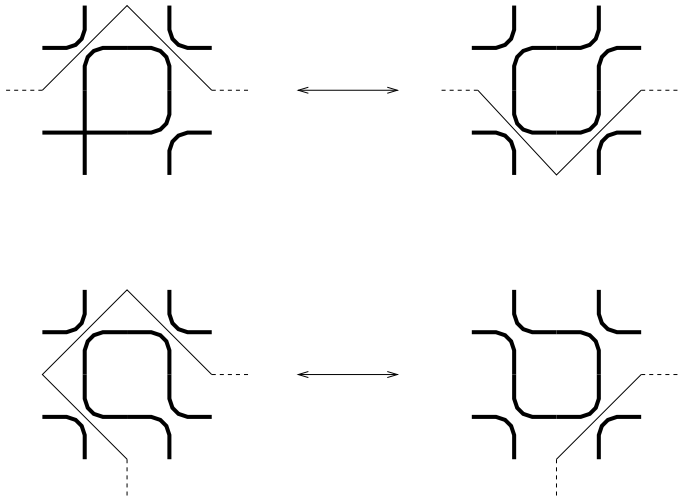

Figure 12: Two examples of plaquette flips which alter locally the interface Γ (Γ is represented as a thin line).

4. Test whether the new loop configuration still admits an interface. If it is the case, denote l' the length of the new interface. If not, reject the step and skip to a new iteration.

5. Perform the local change $\beta \to \beta'$ on P with probability :

$$W(\beta \to \beta') = \begin{cases} \frac{x^{N_c(\beta')} w^{l'}}{x^{N_c(\beta)} w^{l}} & \text{if } x^{N_c(\beta')} w^{l'} < x^{N_c(\beta)} w^{l} \\ 1 & \text{otherwise} \end{cases} \tag{21}$$

This algorithm is able to modify locally the interface, when the plaquette picked at step 1 is close to the interface. Examples of this process are given in figure 12.

6.3 Characteristic times

The Metropolis algorithm described above defines a Markov chain on the set of one-loop configurations with an interface : $(\mathcal{L}_0, \mathcal{L}_1, \ldots \mathcal{L}_K)$. We are interested in the calculation of an observable :

$$\langle A \rangle = \frac{\sum_{\mathcal{L}} \Pi(\mathcal{L}) A(\mathcal{L})}{\sum_{\mathcal{L}} \Pi(\mathcal{L})} \tag{22}$$

where the sums are over one-loop configurations with an interface. The Markov chain is used to build an estimator for this quantity :

$$\bar{A}_{k_0,Q,\tau} = \frac{1}{Q} \sum_{q=0}^{Q-1} A\left(\mathcal{L}_{k_0+q\tau}\right) \tag{23}$$

If the configurations $\mathcal{L}_k$ were independent and obeyed the equilibrium distribution $\Pi(\mathcal{L})$, then the first two moments of the estimator $\bar{A}_{k_0,Q,\tau}$ would be :

$$\langle \bar{A}_{k_0,Q,\tau} \rangle = \langle A \rangle \tag{24}$$

$$\langle \left[\bar{A}_{k_0,Q,\tau} - \langle A \rangle \right]^2 \rangle = \frac{1}{Q} \langle [A - \langle A \rangle]^2 \rangle \tag{25}$$

where the brackets denote averaging with respect to the distribution $\Pi(\mathcal{L})$. The parameters introduced in equation (23) play the following roles :

- The initial time k_0 is the number of configurations to discard at the beginning of the Markov chain. Indeed, the first configurations do not obey the equilibrium distribution $\Pi(\mathcal{L})$. The value of k_0 must be greater than the *equilibration time* of the observable A under the process.
- The time interval τ allows us to discard redundant information arising from non-independent configurations $\mathcal{L}_k$, $\mathcal{L}_{k+1}$, *etc* [19]. One has to choose a value τ greater than the *auto-correlation time* of the observable A under the process.
- The number of samples Q controls the accuracy of the estimator. If the interval τ is large enough, the error on $\langle A \rangle$ is proportional to $Q^{-1/2}$.

In order to determine the equilibration time and the auto-correlation time for the observables of interest, we make a specific hypothesis. The observables we want to compute depend only on the interface. We define the "interface overlap function" :

$$S_\Gamma(\mathcal{L}, \mathcal{L}') = 2 \times \frac{\text{length of } (\Gamma \cap \Gamma')}{l + l'} \tag{26}$$

The hypothesis is that characteristic times for observables depending only on the interface are bounded by a typical timescale associated with the decay of $S_\Gamma(\mathcal{L}_0, \mathcal{L}_\tau)$ as a function of τ. This decay is well described by the auto-correlation function :

$$\phi_\Gamma(\tau) = \frac{S_\Gamma(\mathcal{L}_0, \mathcal{L}_\tau) - S_\Gamma(\mathcal{L}_0, \mathcal{L}_K)}{1 - S_\Gamma(\mathcal{L}_0, \mathcal{L}_K)} \ , \quad K \to \infty \tag{27}$$

This function is plotted in figure 13. The time unit used for plotting is one Monte-Carlo sweep (mcs), corresponding to L^2 elementary iterations of the Metropolis algorithm.

6.4 Ergodicity

The Markov chain $(\mathcal{L}_0, \mathcal{L}_1, \dots)$ defined by the Metropolis procedure converges to the equilibrium distribution $\Pi(\mathcal{L})$ under two conditions : detailed balance and ergodicity. A Markov process is said ergodic if and only if for any pair of configurations $(\mathcal{L}, \mathcal{L}')$, there exists a path of transitions, going from $\mathcal{L}$ to $\mathcal{L}'$, with non-zero transition probability :

$$\mathcal{L} \to \mathcal{L}_1 \to \mathcal{L}_2 \to \dots \mathcal{L}_k \to \mathcal{L}' \tag{28}$$

For the two versions of the algorithm, we do not have any proof of ergodicity for a system of arbitrary size. Nevertheless, we have been able to check exactly the ergodicity property for systems of size $L = 2, 4$. The transfer-matrix algorithm is used to count the number of allowed configurations for small width L. The Metropolis algorithm is modified to visit every configuration obtained by a sequence of local changes, starting from an arbitrary configuration. We find that every allowed configuration is reached by the process. Table 2 gives the number of one-loop configurations on a $L \times L$ square, for the two cases.

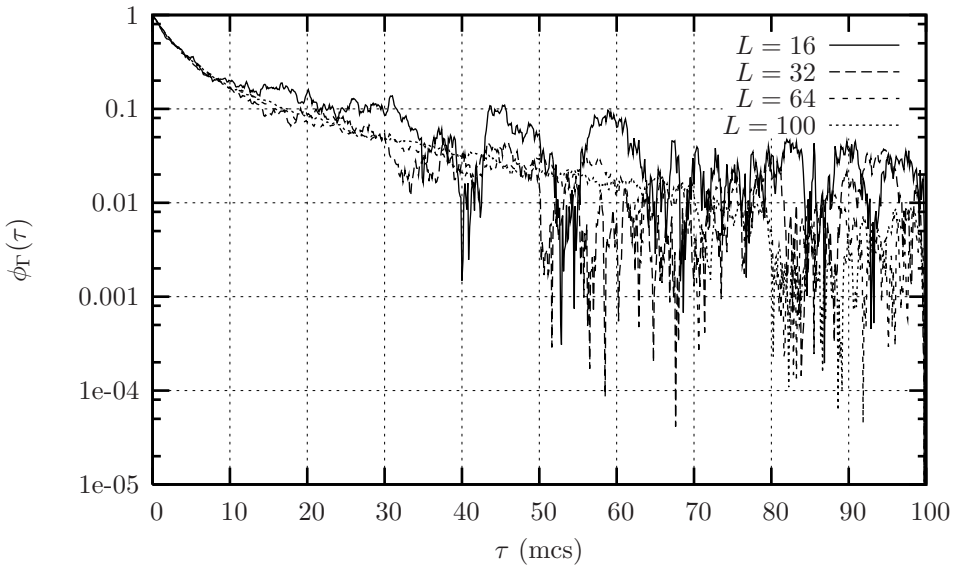

Figure 13: Auto-correlation function $\phi_\Gamma(\tau)$ for parameters $x = 1$, $w = 2$. The initial time was set to $k_0 = 100$ mcs.

L	$\mathcal{N}_{1\,\mathrm{loop}}$	$\mathcal{N}_{1\,\mathrm{loop},1\,\mathrm{interface}}$	ergodicity checked
2	40	32	×
4	5 373 952	3 072 000	×
6	4 380 037 227 741 184	1 705 236 234 240 000	

Table 2: Ergodicity check of the Metropolis algorithms for small system sizes.

6.5 Numerical results

Using Monte-Carlo simulations for various system sizes $L = 16, \ldots, 128$, with the parameters :

$$\begin{aligned} k_0 &= 100 \text{ mcs} \\ \tau &= 100 \text{ mcs} \\ Q &= \begin{cases} 1000 \text{ samples} & \text{for } L < 128 \\ 100 \text{ samples} & \text{for } L = 128 \end{cases} \end{aligned}$$

we estimate the average length $\langle l \rangle$ of the interface Γ, and its fluctuations. We obtain an evidence (see figures 14 and 15) for the scaling laws :

$$\langle l \rangle = L^{1/\nu} H_1 \left([w - w^*(L)] L^{1/\nu} \right) \tag{29}$$

$$\langle \Delta l^2 \rangle = \langle l^2 \rangle - \langle l \rangle^2 = L^{2/\nu} H_2 \left([w - w^*(L)] L^{1/\nu} \right) \tag{30}$$

where $w^*(L)$ is the "finite-size critical point", and H_1, H_2 are scaling functions. The function $H_1(u)$ is increasing on the real line, and the function $H_2(u)$ has a maximum at $u = 0$. We define $w^*(L)$ as the value of the parameter w which maximizes the fluctuation amplitude $\langle \Delta l^2 \rangle$. The maximum of the quantity $\langle \Delta l^2 \rangle$ is expected to follow the scaling law :

$$\langle \Delta l^2 \rangle_{\max} \propto L^{2/\nu} \tag{31}$$

This scaling law is confirmed by the numerical simulation,as shown in figure 16. The numerical fit leads to :

$$1/\nu = 1.28 \pm 0.018 \tag{32}$$

6.6 Scaling laws for the interface

We interpret the scaling laws for the length l of the interface, using the scaling hypothesis for the partition function, close to the critical point $w = w^*$. Suppose that the partition function $Z(N|0, \mathbf{r})$ is a two-point correlation function in some critical field theory. In this theory, the correlation length ξ is related to the deviation from the critical point by :

$$\xi \propto |w - w^*|^{-\nu} \tag{33}$$

The function $Z(N|0, \mathbf{r})$ defines the anomalous dimension η :

$$Z(N|0, \mathbf{r}) = \frac{1}{r^{d-2+\eta}} g(r/\xi) \tag{34}$$

where $d = 2$ is the space dimension, and g is a scaling function. The partition function $Z(N|0, \mathbf{r})$ is also the generating function for the length l of the interface going from 0 to $\mathbf{r}$:

$$\langle l \rangle = \frac{\partial \log Z(N|0, \mathbf{r})}{\partial \log w} = r^{1/\nu} h_1(r/\xi) \tag{35}$$

$$\langle \Delta l^2 \rangle = \frac{\partial^2 \log Z(N|0, \mathbf{r})}{\partial (\log w)^2} = r^{2/\nu} h_2(r/\xi) \tag{36}$$

where the scaling functions h_1, h_2 can be expressed in terms of the function g. So, in particular, the fractal dimension of the interface at the critical point is $d_f = 1/\nu = 1.28$.

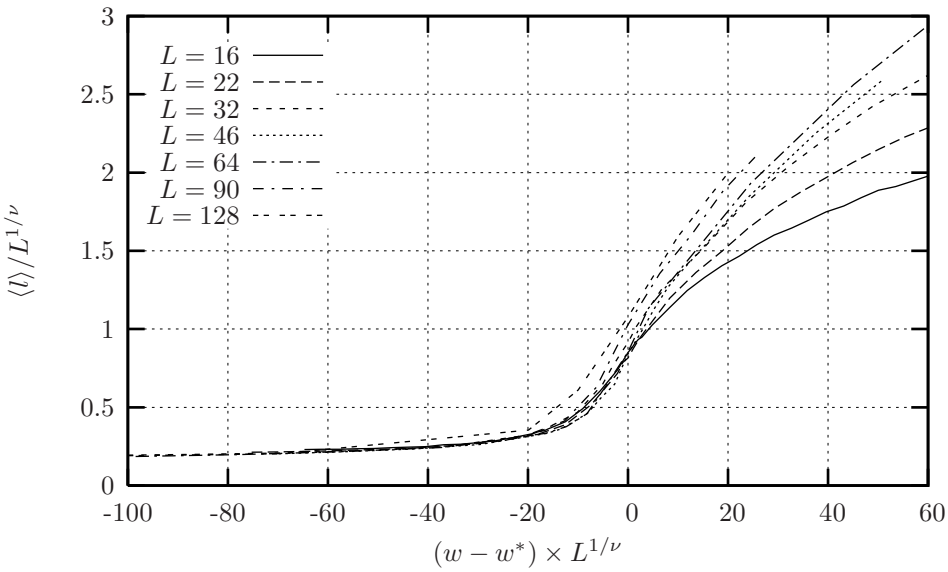

Figure 14: Mean length $\langle l \rangle$ of the interface, as a function of w, for $x = 1$. The parameters $\{w^*(L)\}$ and ν are determined by the maximum of $\langle \Delta l^2 \rangle$ (see figure 16).

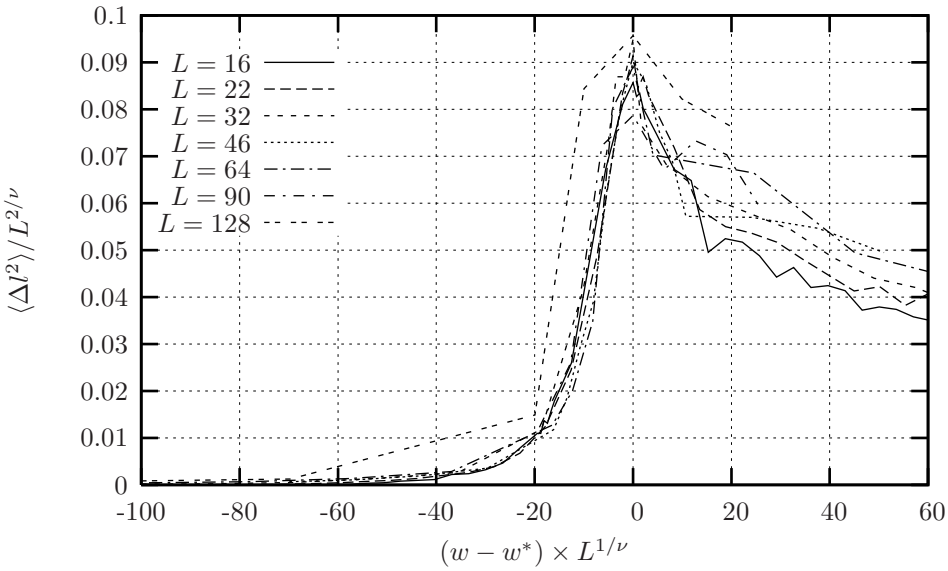

Figure 15: Fluctuations of the length l of the interface, as a function of w, for $x = 1$. The parameters $\{w^*(L)\}$ and ν are determined by the maximum of $\langle \Delta l^2 \rangle$ (see figure 16).

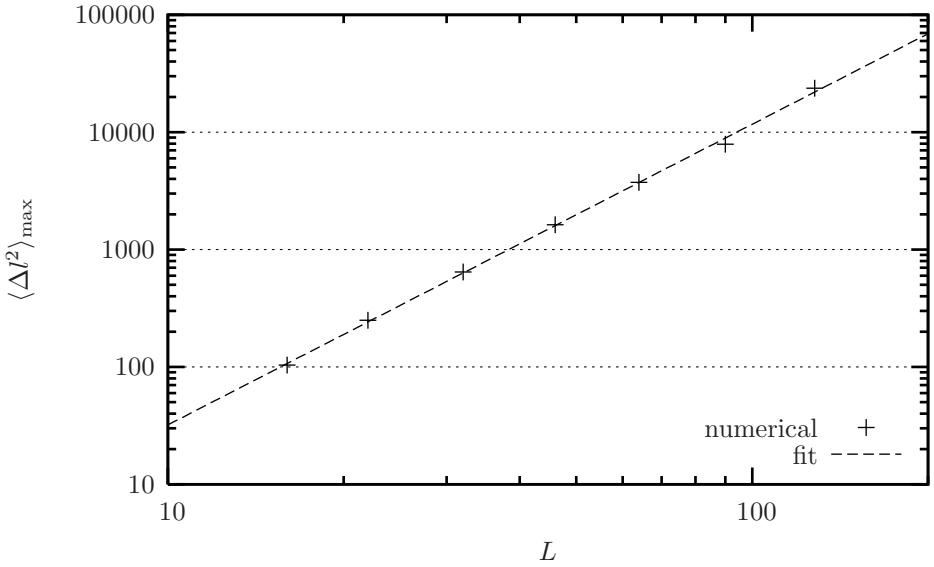

Figure 16: Maximum value of the fluctuations of the length l of the interface, as a function of the system size L. The linear fit gives $\langle \Delta l^2 \rangle_{\max} \propto L^{2/\nu}$, with $1/\nu = 1.28$.

This result can be compared with the transfer-matrix calculations of the exponents $X_{(n_1,n_2)}$. As for the case of polymers [10, 13], the thermal exponent ν is related to the "two-leg exponent" $X_{(0,2)}$:

$$X_{(0,2)} = 2 - \frac{1}{\nu} \tag{37}$$

Indeed, the exponent $X_{(0,2)}$ corresponds to the insertion of two interfaces. According to this argument, the estimated value of $X_{(0,2)}$ (see table 1) gives a fractal dimension :

$$d_f = 1.2 \pm 0.02 \tag{38}$$

This estimate of ν is only marginally compatible with (32), but this was to be expected given the difficulty in estimating reliable error bars within the transfer matrix method.

7 Conclusion

In Brownian motion, the fractal dimension of the boundary is known to be $D_f = 1/\nu = 4/3$, a celebrated conjecture of Mandelbrot's, established rigorously by Lawler, Schramm and Werner [2].[2] At the critical value of w where the interface is allowed to grow in our fully packed trail model, the result (32) is quite close to this value. Since by construction Γ is self avoiding, and since few universality classes are known for self-avoiding walks (even though the background of trails induces non local interactions in Γ) it is tempting to speculate that our $\nu = 3/4$ indeed.

[2] We note that in this case there is no microscopic duality between the non-intersecting Brownian walk and any sort of "interface", since the Brownian walk is not forced to fill up space. It would be interesting to see if any such interface can be defined.

In the context of Brownian motion, the problem closest to ours is the problem of non-intersections of packets of walks. We shall restrict to situations with packets made of one or two walks only. Suppose we have n_1 walks and n_2 pairs of walks, and suppose we demand that no intersection occurs between either sets, while for each pair of walks in the set n_2, intersections are allowed. The exponent is then known to be [2] :

$$x = 2\zeta(n_1, n_2) = \frac{m^2 - 1}{12} \tag{39}$$

where :

$$m = 2n_1 + 3n_2 \tag{40}$$

One recovers the usual case of non-intersection exponents when $n_2 = 0$, $n_1 \equiv L$ in Duplantier's notations [3] (not to be confused with L the system size in this paper).

Assuming (without clear justification) that similar properties might hold for the non-intersection exponents of trails, we found that the following empirical formula :

$$x = \frac{m^2 - 1}{12}, \qquad m = \frac{3}{2}n_1 + 2n_2 - 1 \tag{41}$$

gives a decent fit to our data, as mentioned in section 5.6.

Recall that the numerical data used to obtain this conjecture are affected by very bad convergence properties. An analytical approach and further numerical confirmation are needed to make progress on the problem. For example, one may think of attacking the problem using quantum gravity methods.

An important point concerns the value of n (the loop fugacity) that is best suited for comparison with Brownian motion. We chose in this paper $n = 0$ mostly by analogy with the usual SAW case, but notice that formally the corresponding central charge is $c = -1$ [7]. This might not be the best choice, since non-intersection exponents such as (39) appear in a CFT with $c = 0$ [5, 3]. On the other hand, the value $c = -1$ is really a property of the "bulk" of dense trails, and it is not excluded that their frontiers might be described by a different CFT. In fact, it might well be that non-intersection exponents are independent on the value of n—after all, the dense trail models with $n < 2$ have properties which, in many respects, are independent of n (such as the fuseau exponents, which are all vanishing [7]). Some thoughts on the proper generalization of the lattice model needed to deal with the case $n \neq 0$ are presented in the Appendix below. We hope to get back to this question soon.

Acknowledgements
One of the authors (YI) thanks B. Nienhuis and W. Kager for their hospitality at the ITFA, and for interesting discussions on generalizations to $n \neq 0$. Discussions with M. Bauer, B. Duplantier and S. Majumdar (from whom we learned about the known results on the point (4) of figure 5) are also gratefully acknowledged.

Appendix : Ideas for generalizations to $n \neq 0$

In the planar geometry, when n is non-zero, several loops are allowed to cover the lattice, so the interface defined in section 3 is no longer unique.

In the case $n = 0$, the coloring of loops with two colors was used in section 5 to express with local weights the existence of an interface. When n is non-zero, this trick can inspire some generalizations of the problem. These are best defined on a cylinder.

Let Z_{col} be the partition sum of the model defined by the vertices weights of figure 9, and the non-local weight n for each closed loop. Given a particular configuration $\mathcal{L}$ consisting of several uncolored loops, the model allows

several colorings of $\mathcal{L}$. Intersections among the loops of $\mathcal{L}$ define a partition into *packets* of mutually intersecting loops. Packets may be colored independently in two ways, but loops belonging to the same packet must have the same color. Thus, the number of such objects appears in the partition sum :

$$Z_{\rm col}(M,L) = \sum_{\mathcal{L}} \left(\prod_i w_i \right) n^{\#\rm loops}\ 2^{\#\rm packets} \tag{42}$$

where the sum is over uncolored loop configurations, and the first factor stands for the local weights of figure 9.

If a change of colors is imposed when the boundary is crossed, then no packet is allowed to wrap around the cylinder. This is equivalent to the existence of an interface as defined in figure 8. So, like in the case $n = 0$, this model is able to express locally the existence of an interface. Unfortunately, we have not been able to define a unique interface, so we cannot control its length l like in the previous case.

A special case is when $x = 0$. Then a packet is identical to a loop, and the partition sum becomes :

$$Z_{\rm col}(M,L) = \sum_{\mathcal{L}} \left(\prod_i w_i \right) (2n)^{\#\rm loops} \quad (x=0) \tag{43}$$

Note that this model contains the Potts model as a particular case, when $w = 1$.

The form (42) of the partition sum of the colored loop model suggests another generalization of the previous models, obtained by introducing a second non-local weight m for each packet of closed loops :

$$Y(x,n,m) = \sum_{\mathcal{L}} x^{\#\rm crossings}\ n^{\#\rm loops}\ m^{\#\rm packets} \tag{44}$$

where the sum is over uncolored loop configurations.

NB : In section 3, we saw that when $(n,m) = (0,2)$, the model with an interface is not critical. However, it may be possible to define a limit $n \to 0$ for the partition sum (44), which defines a critical model with an interface.

References

[1] J.L. Jacobsen and H. Saleur, *Conformal boundary loop models*, math-ph/0611078.

[2] G.F. Lawler, O. Schramm and W. Werner, Acta Math. **187**, 237–273 (2001); math.PR/9911084.

[3] B. Duplantier, Phys. Rev. Lett. **81**, 5489 (1998).

[4] D.E. Derkachov, G.P. Korchemsky, A.N. Manashov, JHEP 0310 (2003) 053, and references therein.

[5] B. Duplantier and K.-H. Kwon, Phys. Rev. Lett. **61**, 2514–2517 (1988).

[6] M.S. Cao and E.G.D. Cohen, J. Stat. Phys. **87**, 147 (1997); cond-mat/9608159.

[7] J.L. Jacobsen, N. Read and H. Saleur, Phys. Rev. Lett. **90**, 090601 (2003); cond-mat/0205033.

[8] M.J. Martins, B. Nienhuis and R. Rietman, Phys. Rev. Lett. **81**, 504–507 (1998); cond-mat/9709051.

[9] W. Kager and B. Nienhuis, J. Stat. Mech., P08004 (2006); cond-mat/0606370.

[10] B. Nienhuis, Phys. Rev. Lett. **49**, 1062 (1982).

[11] G. F. Lawler, *Intersections of random walks* (Birkhäuser, Boston, 1996).

[12] I. Jensen, J. Phys. A **37**, 5503–5524 (2004).

[13] B. Duplantier and H. Saleur, Nucl. Phys. B **290**, 291 (1987).

[14] A. Coniglio, Phys. Rev. Lett. **62**, 3054 (1989).

[15] B. Duplantier and H. Saleur, Phys. Rev. Lett. **58**, 2325 (1987).

[16] H.W.J. Blöte, J.L. Cardy and M.P. Nightingale, Phys. Rev. Lett. **56**, 742 (1986); I. Affleck, Phys. Rev. Lett. **56**, 746 (1986).

[17] J.L. Cardy, J. Phys. A **17**, L385 (1984).

[18] K. Binder, D.W. Heermann, *Monte-Carlo Simulation in Statistical Physics*, Springer (1988).

[19] A. Sokal, *Monte Carlo methods in statistical mechanics: foundations and new algorithms*, in *Functional Integration: Basics and Applications (1996 Cargèse Summer School)* ed C. DeWitt-Morette, P. Cartier and A. Folacci (New York: Plenum) pp 131-192 (1997).
http://www.math.nyu.edu/faculty/goodman/teaching/Monte Carlo/Sokal.ps